Geophys. J. Int. (2009) **179,** 18–34 doi: 10.1111/j.1365-246X.2009.04258.x

Palaeomagnetism and geochronology of the Proterozoic dolerite dyke from southwest Greenland: indication of low palaeointensity*

Masako Miki,[1] Aya Taniguchi,[1] Masahiko Yokoyama,[1] Chitaro Gouzu,[2,3] Hironobu Hyodo,[4] Koji Uno,[5] Haider Zaman[1] and Yo-ichiro Otofuji[1]

[1]*Department of Earth and Planetary Sciences, Faculty of Science, Kobe University, Kobe* 657-8501*, Japan. E-mail: makomiki@kobe-u.ac.jp*
[2]*Open Research Center, Okayama University of Science,* 1-1 *Ridai-cho, Okayama* 700-0005*, Japan*
[3]*Hiruzen Institute for Geology and Chronology,* 2–5 *Nakashima, Naka-ku, Okayama* 703-8252*, Japan*
[4]*Research Institute of Natural Sciences, Okayama University of Science,* 1-1 *Ridai-cho, Okayama* 700-0005*, Japan*
[5]*Faculty of Education, Okayama University, Okayama* 700-8530*, Japan*

Accepted 2009 May 18. Received 2009 May 5; in original form 2008 February 28

SUMMARY

Intensity of the geomagnetic field during the Archaean can potentially be used to study an evolution of the dynamo activity in the Earth's core. In order to investigate this issue, we present new palaeomagnetic and geochronological results from the dolerite dyke, which have been intruded into the Archaean Gneisses of Nuuk area, southwest Greenland. $^{40}Ar/^{39}Ar$ dating of the pyroxene grains from dolerite yield an age of 2585 ± 21 Ma. The high temperature component, which has been recognized as a characteristic direction, is identified in 24 dolerite samples. Comparison of the palaeomagnetic directions from dolerite dykes with those from host gneisses suggests a primary origin for this component. Magnetic mineralogical and grain size investigations revealed a pseudo-single domain magnetite as a dominant career of magnetization. Thellier palaeointensity determinations of 14 dolerite specimens yield a mean field value of 13.9 ± 2.5 μT. Strength of the virtual dipole moment (2.30 ± 0.42 × 10^{22} Am^2) obtained from this study is about one quarter of the present Earth's filed value. A simulation based numerical model of the Thellier experiments suggests that the presence of multidomain grains can play a role in enhancing the strength of palaeointensity. Even after taking in to account the effects of multidomain grains, an intensity value (13.9 μT) from this study suggests that the strength of geomagnetic field at about 2.6 Ga was much lower than that of the present time.

Key words: Palaeointensity; Rock and mineral magnetism; Arctic region.

1 INTRODUCTION

Palaeointensity of the geomagnetic field during the Archaean and Proterozoic have been recognized as a key to improve our knowledge about the formation of the inner core and the start of geo-dynamo. Using the parameters and calculations from the Earth's thermal history (e.g. Stevenson *et al.* 1983; Breuer & Spohn 1995) it has been suggested that growth of the inner core during the early days of the Earth's history have instigated the process of geo-dynamo. First compilation of the palaeointensity data from the Archaean and Proterozoic by Hale (1987) was interpreted as being consistent with sharp increase in the geomagnetic intensity at about 2.7 Ga; however, some of these data are still questionable in terms of their age and/or palaeomagnetic reliability criteria. Although, some new palaeointensity data have been added (e.g. Smirnov *et al.* 2003; Macouin *et al.* 2006) and some have been reinvestigated (Yoshihara & Hamano 2004; Smirnov & Tarduno 2005), the available data are still not sufficient to fully resolve this issue. Therefore, an accumulation of additional palaeointensity and radiometric age data were greatly needed to document changes in the strength of geomagnetic field and enhance our understanding about the growth of geo-dynamo.

Keeping in view this demand for further investigations, we present new palaeointensity results together with radiometric dating from the Archaean craton of southwest Greenland. For this purpose, samples are collected from basic dykes, which provide fresh information about the behaviour of geomagnetic field prior to the formation of modern geodynamo system.

2 GEOLOGY OF THE STUDY AREA AND SAMPLING PROCEDURE

The Nuuk region of western Greenland is characterized by the Archaean Gneiss complex, which has been radiometrically dated between 3800 and 2800 Ma (Escher & Watt 1976; Nutman *et al.* 1989). This area is believed to have experienced an amalgamation of

*Correction added after online publication 2009 July 22: 'southeast' has been corrected to 'southwest'.

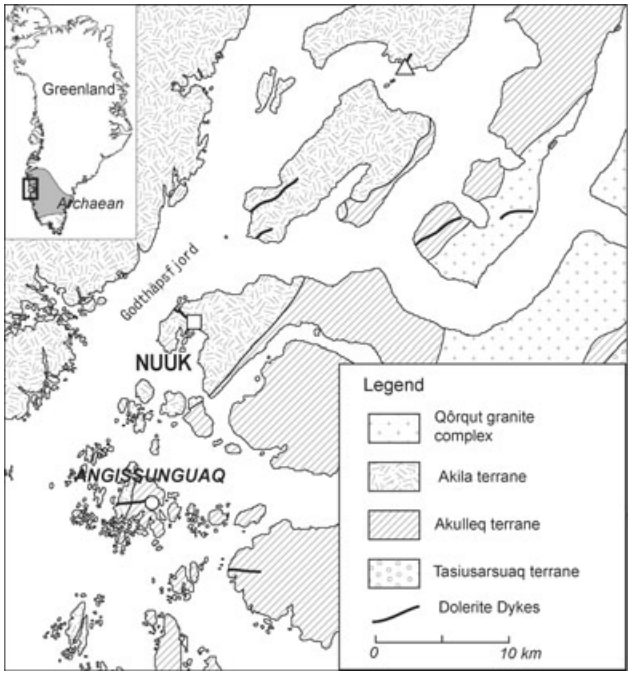

Figure 1. Simplified geological map of southwest Greenland after Friend *et al*. (1996). An open circle indicates our sampling locality. Granitic dyke with age of 2712 Ma (Friend *et al*. 1996) is indicated by a triangle. A square sign indicate another doleritic dyke of 2752 Ma age (Morimoto *et al*. 1997).

independently evolved crustal terranes at about 2720 Ma (Friend *et al.* 1988, 1996). From northwest to southeast, these terranes are classified as: the predominant late Archaean Akia Terrane; the Akulleq Terrane (containing both the early and late Archaean rocks); and the late Archaean Tasiusarsuaq Terrane (Fig. 1).

The basic dykes, collectively named as a metadolerite (MD) dyke swarm (Bridgewater *et al.* 1976), are abundant in the Archaean craton of southwest Greenland. Major dolerite swarms were emplaced into the Archaean gneisses after the end of plutonic activity (at about 2700–2500 Ma), which is much earlier than the time assigned to the development of Ketilidian mobile belt at about 1850 Ma (Nielsen 1985). An isochron (Rb-Sr) age of 2130 Ma has also been reported from a dyke in southwestern part of the craton (Kalsbeek & Taylor 1985). Many of these dykes are 20–100 m wide and up to several tens of kilometres long.

Although, these dykes in the Nuuk area have been named as MD dykes, most of them are well preserved without any obvious metamorphic signature. K-Ar age of 2752 Ma has been reported from a dyke in the Nuuk town (Morimoto *et al.* 1997). Field observation of another dyke, which is located at about 15 km south of the Nuuk town on a small island of Angissungaq, shows clear signs of being intruded into the host gneisses (Fig. 1). This dyke (up to 3.5 km long), which has penetrated the host rock at a boundary between the Akila and Akulleq terranes, generally follow an east–west trending attitude.

Dolerite samples oriented with sun compass were drill-cored at two sites. These sites are located at 5 m distance from each other along the contact zone with host rocks. More than 17 samples were drilled from each site. Three large block samples oriented with magnetic compass were also collected for palaeomagnetic study. Slightly away from the contact zone, several block samples were collected for geo-chronological investigations.

In order to carry out baked contact test, samples were collected from the host rocks (gneisses) at three different localities, that is, two sites (GP83, GP84) from the contact zone; one (GP86) at 5 m from the contact zone, and another (GP 85) at 16 m from the contact zone.

3 GEOCHRONOLOGY

We have carried out $^{40}Ar/^{39}Ar$ dating of the samples with abundant plagioclase and clinopyroxene grains.

3.1 Sample description

Very fresh dolerite sample (GP-80) was selected for geochronological investigations. This sample, which is composed of plagioclase, clinopyroxene and olivine/opaque minerals, shows a typical ophitic texture with medium grain size (*ca*. 1.2 mm). Although, the studied sample looked quite fresh, weak secondary alteration has been found under microscopic observation that in turn produced small amount of chlorite, biotite and clay minerals. In some plagioclase grains, this secondary alteration is recognized by pale-brown smoky colour, particularly in the core part.

3.2 Sample preparation for geochronological study

About 1-cm-thick slices of dolerite sample were prepared for geochronological investigations. In order to avoid contaminations from wall rocks or xenoliths, rock-cutter was used for sample preparation. Dried sample was then crushed and sieved in a #20–40 and #150–200 mesh size. Plagioclase and clinopyroxene grains were separated by magnetic separator. Following this, purifications and final selections of grains were made through hand-picking under the binocular microscope.

3.3 $^{40}Ar/^{39}Ar$ age analyses

$^{40}Ar/^{39}Ar$ dating of the individual plagioclase and clinopyroxene grains was carried out using the step-heating method. This method was applied to four clinopyroxene and two plagioclase crystals of about 0.5 mm in size. Each crystal was placed in a hole (2 mm) drilled on aluminum tray together with standard age sample (3 gr hornblende; Roddick 1983). Additionally, calcium ($CaSi_2$) and potassium salts (synthetic $KAlSi_3O_8$ glass) were also placed on tray for Ca and K corrections. Subsequently, the tray was vacuum-sealed in a quartz tube. Samples were then exposed to Neutron radiation for 8 hours in the core of 3 MW Research Reactor of Kyoto University (KUR) using the hydraulic rabbit facility (sample-capsule transferring system with hydraulic pressure). The fastest neutron flux density was 3.9×10^{13} n cm^{-2} s, which is confirmed to have been stayed uniform in the dimension of the sample holder (diameter 16 mm $\times$ height 15 mm), as little variation in the J-value of evenly spaced age standards has been observed (Hyodo *et al*. 1999). An averaged J-value and correction factors for potassium and calcium are $J = 0.0041759 \pm 0.0000201$ ($^{40}Ar/^{39}Ar$) K $= 0.0186 \pm 0.0035$, ($^{36}Ar/^{37}Ar$) Ca $= 0.000260 \pm 0.000014$ and ($^{39}Ar/^{37}Ar$) Ca $= 0.000716 \pm 0.000016$, respectively.

Each crystal was analysed by stepwise-heating technique using the 5 W continuous argon ion laser. Following this procedure, crystals were heated under the defocused laser beam at a given temperature for 30 s. The sample temperature was monitored by an infrared thermometer, which have a precision of 3 °C within an area of 0.3 mm diameter (Hyodo *et al.* 1995). An extracted gas was purified with a SAES Zr-Al getter (St 101), which has been kept at 400

Table 1. $^{40}Ar/^{39}Ar$ analytical data of pyroxenes in sample GP-80.

Temperature (°C)	Cum. ^{39}Ar	$^{40}Ar_{Atm}$(per cent)	$^{40}Ar*/^{39}Ar_K$	$^{37}Ar_{Ca}/^{9}Ar_K$	Age (Ma)
GP80CPX01 (clinopyroxene)				*J*-value: 0.0041759 ± 0.0000201	
597	0.011	1.48	9202.2 ± 1753.0	8.014 ± 10.397	6629 ± 335
704	0.045	1.22	7222.6 ± 599.6	20.335 ± 3.914	6205 ± 145
803	0.097	1.24	1933.7 ± 121.3	11.373 ± 2.425	3979 ±101
895	0.195	0.34	777.6 ± 30.6	2.368 ± 1.068	2609 ± 55
943	0.292	0.61	786.2 ± 24.6	4.750 ± 1.309	2624 ± 44
999	0.416	0.31	760.0 ± 16.3	2.940 ± 0.955	2578 ± 30
1040	0.534	1.27	738.7 ± 20.7	2.469 ± 1.215	2539 ±39
1096	0.718	1.20	969.2 ± 11.1	7.782 ± 0.696	2921 ± 18
1114	0.809	1.33	1861.9 ± 71.0	47.893 ± 2.584	3918 ± 61
Fused	1.000	1.86	1456.9 ± 35.4	202.081 ± 5.508	3532 ± 38
				Total age	3473 ± 17 Ma
		Plateau age (895–1040 °C, 43.7 per cent of ^{39}Ar released)			2585 ±21 Ma
GP80CPX 02 (clinopyroxene)				*J*-value: 0.0041759 ± 0.0000201	
599	0.015	0.78	12399.0 ± 928.6	7.539 ± 1.541	7155 ± 133
708	0.062	0.73	6661.4 ± 197.7	16.388 ± 0.862	6063 ± 52
803	0.143	0.66	1451.1 ± 22.7	10.685 ± 0.717	3526 ± 25
898	0.272	0.48	1029.5 ± 13.5	4.274 ± 0.331	3008 ± 20
946	0.372	0.78	886.6 ± 12.7	2.705 ± 0.434	2793 ± 21
999	0.477	0.30	1001.4 ± 13.3	3.704 ± 0.573	2968 ± 21
1047	0.584	0.47	1229.4 ± 17.8	2.929 ± 0.433	3272 ± 23
1069	0.639	0.41	1938.0 ± 42.5	6.342 ± 0.682	3983 ± 36
Fused	1.000	0.59	2271.8 ± 20.3	28.366 ± 0.444	4240 ± 17
				Total age	4032 ±11 Ma
GP80CPX 03 (clinopyroxene)				*J*-value: 0.0041759 ± 0.0000201	
594	0.004	0.94	61521.0 ±57753.0	14.983 ±65.140	10017 ± 1687
704	0.060	0.40	7688.0 ± 566.3	16.998 ± 3.993	6314 ± 129
809	0.166	1.04	1793.7 ±69.9	10.258 ± 2.079	3859 ± 62
896	0.331	0.11	765.4 ± 17.0	5.299 ± 1.131	2587 ± 31
946	0.399	0.00	955.1 ± 41.7	6.139 ± 2.223	2899 ± 63
990	0.481	0.00	993.5 ± 48.7	0.000 ± 0.000	2956 ± 72
1044	0.604	0.63	1411.0 ± 61.6	0.468 ± 2.183	3483 ± 68
1130	0.668	0.69	3297.6 ± 236.1	8.420 ± 3.572	4858 ± 121
Fused	1.000	0.70	2546.8 ± 46.2	33.775 ± 1.170	4427 ± 31
				Total age	4312 ± 23 Ma
GP80CPX04 (clinopyroxene)				*J*-value: 0.0041759 ± 0.0000201	
596	0.000	0.82	590940 ± 2655400	203 ± 1052	14092 ± 8104
708	0.020	0.99	13242.0 ± 670.5	40.323 ± 5.431	7272 ± 90
802	0.071	0.92	1992.8 ± 77.1	8.523 ± 2.149	4027 ± 63
895	0.179	0.93	1182.6 ± 17.8	3.604 ± 0.948	3214 ± 24
953	0.325	0.74	836.8 ± 12.9	3.067 ± 0.623	2711 ± 23
999	0.480	0.46	731.1 ± 13.2	3.015 ± 0.583	2525 ± 25
1048	0.665	0.59	890.4 ± 12.4	1.868 ± 0.422	2799 ± 21
1098	0.805	0.73	1944.0 ± 40.2	3.612 ± 0.777	3987 ± 34
1107	0.828	0.94	3790.8 ± 242.1	12.990 ± 2.736	5093 ± 109
1200	0.884	0.60	3127.9 ± 79.2	20.435 ± 1.755	4769 ± 43
Fused	1.000	0.79	1600.6 ± 23.1	25.020 ± 0.982	3679 ± 24
				Total age	3817 ± 13 Ma

°C for 5 min. Argon isotopes were then measured using a custom-made high-resolution mass spectrometer [$(M/\Delta M) > 400$], which allow separation of the hydrocarbon peaks with the exception of mass 36 (Hyodo *et al.* 1994). Typical blanks of extraction lines for ^{36}Ar, ^{37}Ar, ^{38}Ar, ^{39}Ar and ^{40}Ar are 5×10^{-14}, 3×10^{-14}, 3×10^{-14}, 3×10^{-14} and 2×10^{-12} ccSTP, respectively.

A meaningful age data have been obtained from the clinopyroxene grains. Results of the stepwise heating analyses are listed in Table 1, while age related spectra and $^{37}Ar_{Ca}/^{39}Ar_K$ ratios are shown in Figs 2 and 3.

As shown in Fig. 2 (a typical result of sample CPX01), and listed in Table 1, an age related spectra of four clinopyroxene grains is characterized by saddle-shape graphs. An apparent-age spectra drops from 7.0 Ga (step 1) to *ca*. 2.6 Ga (step 4), and climbs again up to 3.9 Ga (Step 9). The lowermost four steps of age spectrum exhibit a laugh plateau age of 2585 ± 21 Ma, which hold 44 per cent of the total ^{39}Ar released. In these steps, the ratio of $^{37}Ar_{Ca}/^{39}Ar_K$ exhibits constant value of *ca*. 3, indicating a uniform phase during the release of ^{37}Ar, ^{39}Ar and ^{40}Ar. Plot in Fig. 3 shows a comparison between all four clinopyroxene grains, where U-shaped spectrum is consistently displayed. An intermediate flat steps in this figure yield visible concordance in ages, where the youngest age of the saddled bottom converges with the lowermost bottom of the CPX04 (2525 ± 25 Ma). The $^{37}Ar_{Ca}/^{39}Ar_K$ ratios of the corresponding steps

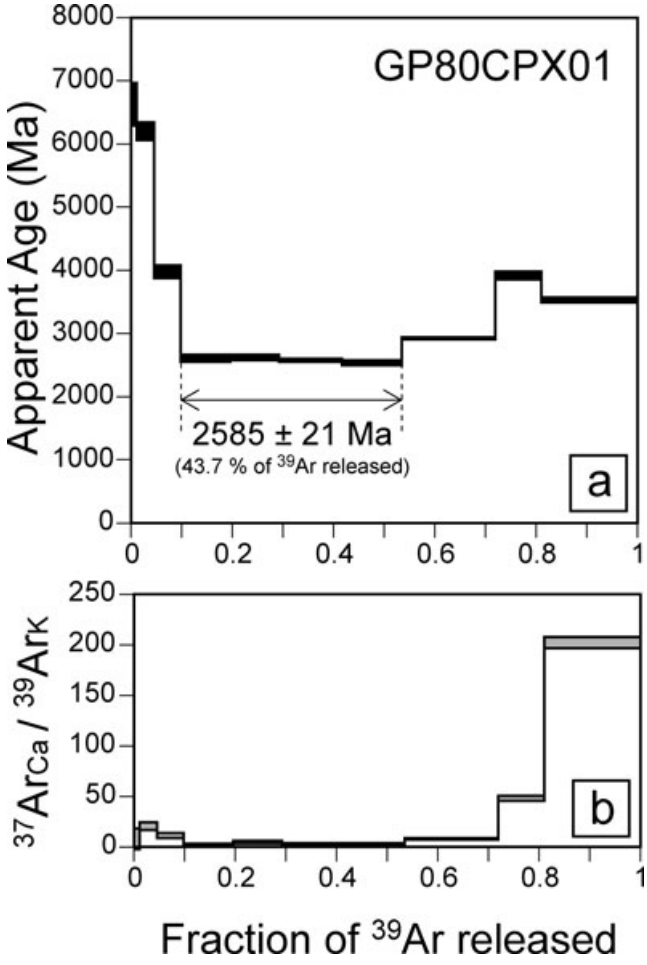

Figure 2. A Typical example of $^{40}Ar/^{39}Ar$ age spectra and $^{37}Ar_{Ca}/^{39}Ar_K$ ratio for clinopyroxene crystal (GP80CPX01) using step-heating analyses.

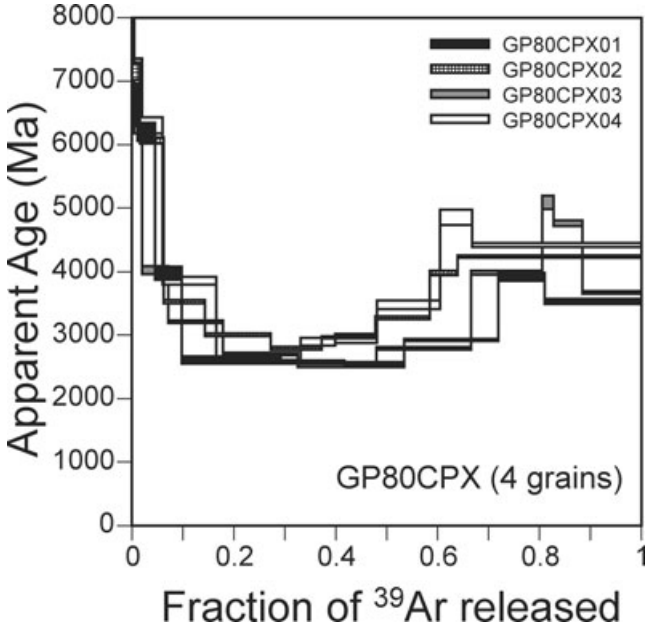

Figure 3. Comparison of the $^{40}Ar/^{39}Ar$ age spectra for all 4 clinopyroxene crystals (GP80CPX01, GP80CPX02 GP80CPX03 and GP80CPX04).

at youngest age show stable values around *ca.* 3 for all four grains, indicating an occurrence of degassing from the same mineral phase in clinopyroxenes. Whilst, the low- and high-temperature phases in the apparent-age spectra are attributed to the release of excessive argon from clinopyroxene, it looks hard to determine geologically meaningful ages from these results. However, the following three positive facts should be noted in this regard: (1) rocks are fairly fresh with only minor alterations; (2) convergence is observed in the saddle age and (3) stable values are obtained at youngest age level (due to gas released from the same mineral phase in clinopyroxene). These points characterize the convergent related values as a valid age for the studied dyke. Lee *et al*. (1990) have reported almost similar type of convergence in the pyroxene grains extracted from mafic dykes of the Kapuskasing Structural Zone, Canada. They have recovered a dyke intrusion age from the baked contact test, which is in good agreement with the saddle bottom age of the $^{40}Ar/^{39}Ar$ spectra. Thus, an integrated age of 2585 $\pm$ 21 Ma, which we obtained from the largest fraction (CPX01) of four grains, is assigned to be the best estimated age for the studied dolerite dyke.

Comparable age of *ca.* 2752 $\pm$ 63 Ma has also been reported from a dyke swarms located close to the study area (Morimoto *et al.* 1997), which further support this apparent age of 2585 $\pm$ 21 Ma as a time for dyke intrusion.

4 PALAEOMAGNETISM

Six to fourteen cores were drilled from each block sample in the palaeomagnetic laboratory of Kobe University. Cores were further sliced in to specimens of 2.5 cm height. Natural remanent magnetizations (NRMs) were measured by spinner magnetometer. More than 50 specimens were thermally demagnetized in 15 heating steps up to 600 °C. Stepwise alternating field demagnetization (AFD) method was also applied to several specimens. Components of magnetizations were estimated by principal component analysis (Kirschvink 1980).

In case of dolerite dyke, stable high-temperature component is isolated after removing low-temperature component by 400 °C (Fig. 4a). This high-temperature component, which has been unblocked by 580 °C, is recognized as a characteristic remanent magnetization (ChRM). Almost similar trend of this component is identified by AFD method above 20 mT (Fig. 4b). We have successfully obtained ChRM direction from 24 specimens. Fairly small MAD values obtained from these samples (between 2.2° and 6.3°) indicate a straight line like behaviour in the demagnetization curves. As shown in the Fig. 4(c), mean direction of the ChRM component is obtained as $D = 253.0°$, $I = 62.6°$ ($\alpha_{95} = 2.5°$), which is obviously different from the present-day geomagnetic field. Fairly small value of α_{95} indicates an appropriate magnetic cleaning.

In case of host gneisses, stable demagnetization behaviour is observed in the samples of those two sites (GP85 and GP86), which are located at 16 and 5 m from the contact zone, respectively (Fig. 5). A high-temperature component (recognized as a ChRM) is identified above 400 °C, and is unblocked at about 580 °C. This component is successfully isolated from 16 specimens (eight each from GP85 and GP86). Slight difference in directional behaviour between these two sites may be due to the influence of dolerite intrusion (Fig. 6). Directions obtained from site GP86 (located at 5 m from the contact zone) and the dolerite dyke are somewhat closer to each other as compared to that of site GP85 (at 16 m from the contact zone), indicating a positive backed contact test. However, all 16 samples have been used for the calculation of gneiss's mean direction, since

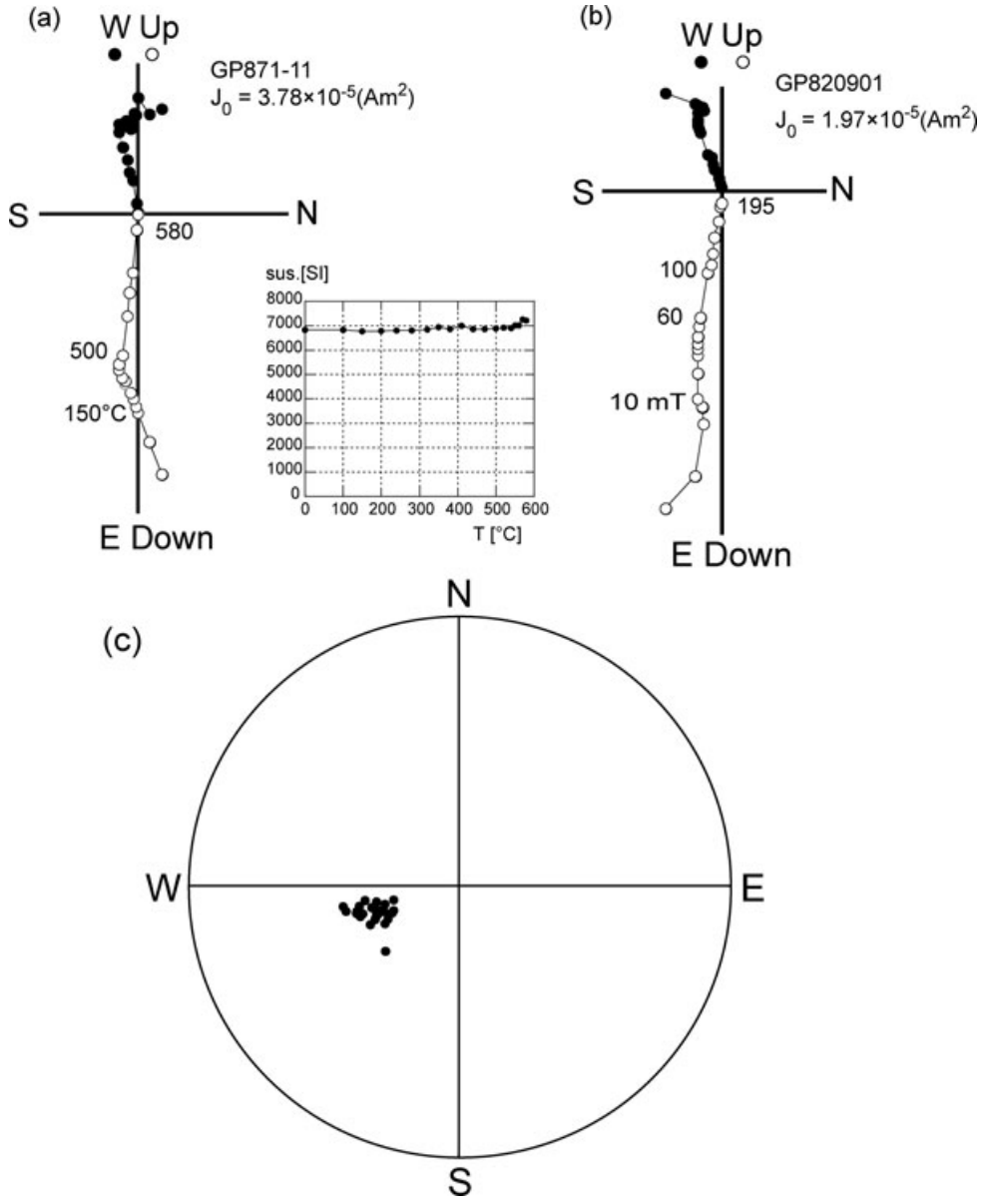

Figure 4. Diagrams of stepwise demagnetization experiments for the dolerite dykes: (a) orthogonal vector endpoint diagram after stepwise thermal (a) and alternating field (b) demagnetization procedure. Variation in magnetic susceptibility after each heating step is also shown in the adjacent diagram. (c) Directions of the high temperature characteristic component for 24 dolerite samples on equal area projection (lower hemisphere).

the available results are only from two sites with negligible difference in behaviour. Mean direction obtained from 16 gneiss samples ($D = 224.6^\circ$, $I = 64.0^\circ$ and $\alpha_{95} = 2.4^\circ$) show a significant difference (by $12.7^\circ \pm 3.1^\circ$) with that from dolerite dyke (Fig. 6c).

This mean direction from host rocks is quite similar to those previously reported (Fahrig & Bridgewater 1976; Morimoto *et al*. 1997) from the Archaean gneiss complex, around the Nuuk town (Fig. 6c and Table 2). Locations of previous studies are situated in the Akia Terrane, which is about 15 km from this study area (Akulleq Terrane). Agreement in palaeomagnetic directions from such a broad area suggests that single geological event seems to have instigated the acquisition of secondary magnetization in the gneisses of both these terranes. Friend *et al.* (1996) have recognized a high-grade metamorphic event at ∼2720 Ma using the SHRIMP U-Pb zircon geochronology, which seems to be the most likely cause of remagnetization in these terranes.

In contrast, palaeomagnetic direction from the dolerite dyke (this study) is not in agreement with previously reported direction of the dolerite dyke from Nuuk Town (Fig. 7, Morimoto *et al.* 1997). A significant difference of $12.0^\circ \pm 5.1^\circ$ between these two sets of directions suggest an acquisition of magnetizations by two separate geological events. These two sets of directions from dolerite dykes are obviously different from that of the host gneisses (Fig. 7). Magnetization of the dolerite dykes appears to have been acquired after the overprinting event in the host gneisses, which we believe is primary in origin (acquired at the time of dyke intrusions), Morimoto *et al*. (1997) has also ascertained an intrusion related magnetization to dolerite dyke using the results of baked contact test.

Gneiss specimens from the contact zone (seven specimens from sites GP83 and GP84) showed fairly different behaviour during the demagnetization procedure. An initial NRM intensity (10^{-9} to 10^{-8} Am^2) is relatively smaller than that of the host gneisses (10^{-8}

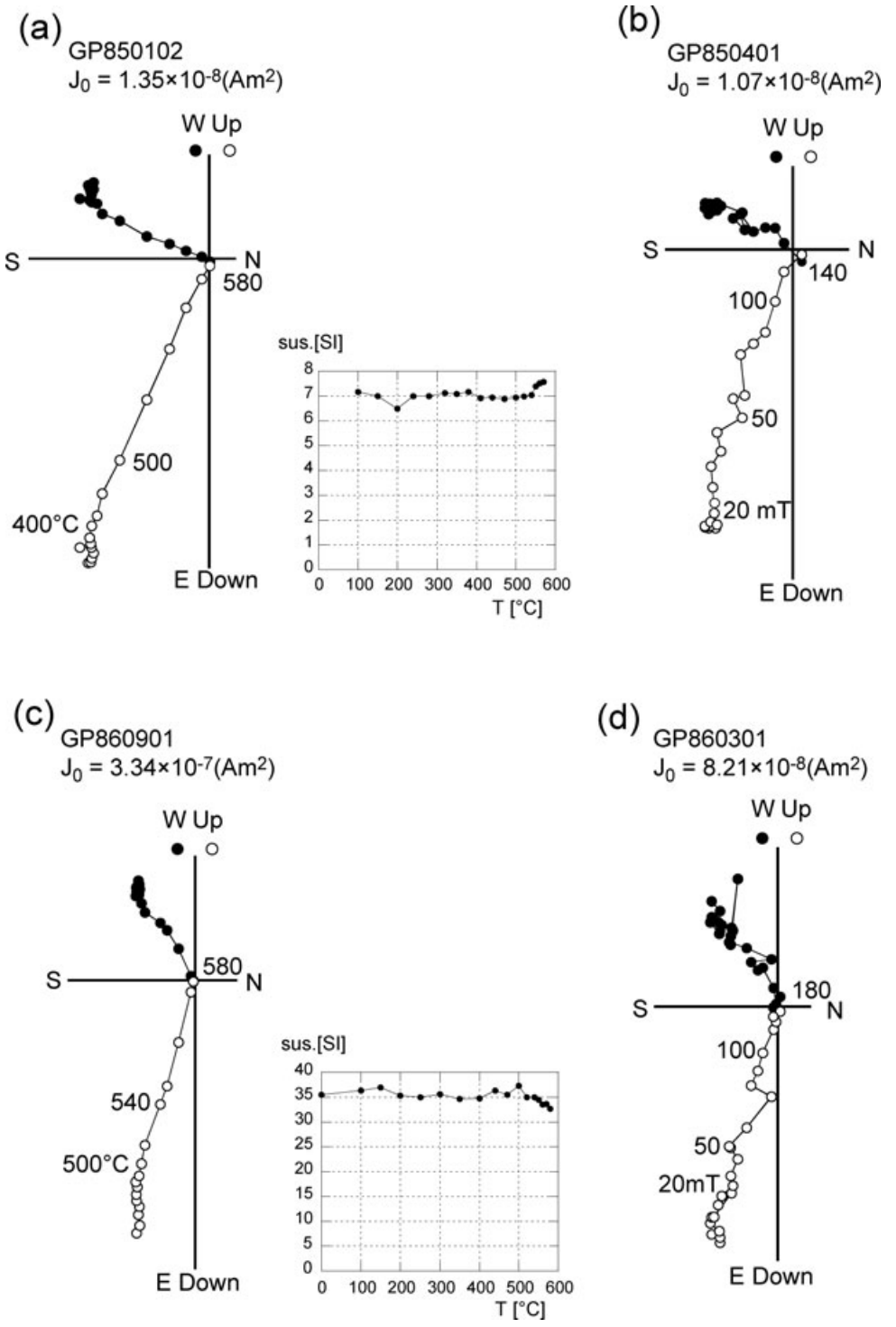

Figure 5. Magnetization behaviour during stepwise demagnetization experiments (both thermal and alternating field) for gneiss samples. (a) and (b) Vector endpoint diagrams for gneiss samples collected at a distance of 16 m from the contact zone; (c) and (d) Vector endpoint diagrams for gneiss samples collected at 5 m from the contact zone. Diagrams showing changes in magnetic susceptibility after each heating step is also given adjacent to (a) and (c).

to 10^{-7} Am^2). The high-temperature component appeared between 400 and 580 °C (Fig. 8). However, due to very weak NRM intensity and unstable demagnetization behaviour, the ChRM component could not be isolated by principal component analysis. We recognized a measured direction after 520 °C demagnetization as a characteristic of high-temperature component and compared the direction with that after some lower temperature demagnetizations (Fig. 9). As evident from equal-area projections, both low and high-temperature components show divergent directional behaviour, indicating the removal of secondary magnetization component to some extent. Palaeomagnetic directions of the high-temperature component after 520 °C are distributed around the mean direction of the

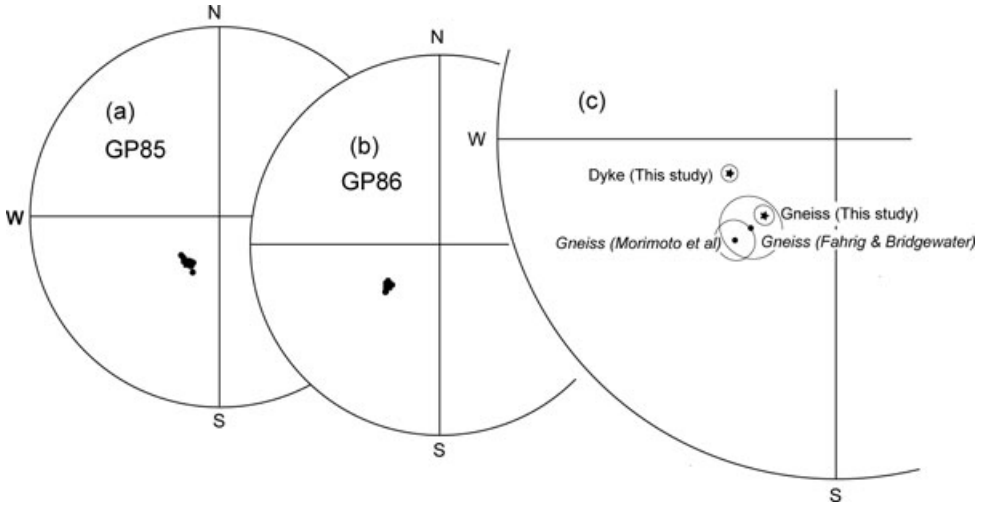

Figure 6. Equal area projections of the high temperature components (ChRM) for gneiss samples and their comparison with previously reported directions: (a) palaeomagnetic directions from site GP85 which is at a distance of 16 m from the contact zone; (b) palaeomagnetic directions from site GP86 which is located at about 5 m from the contact zone and (c) comparison of mean palaeomagnetic direction obtained from 16 samples (sites GP85 and GP86) with those reported from Nuuk gneisses by Morimoto *et al*. (1997) and Fahrig & Bridgewater (1976). Mean direction of the dolerite dyke is also plotted with 95 per cent confidence circle. All projections are on lower hemisphere. Star sign indicate data from this study.

Table 2. Palaeomagnetic directions from Nuuk area.

Description	*N*	Dec (°)	Inc (°)	*k*	α_{95} (°)
Dolerite dyke (this study)	24	253.0	62.6	229.6	2
Dolerite dyke (Morimoto *et al*. 1997)	13	255.4	74.6	–	4.7
Gneiss (this study)	16	224.6	64.6	239.7	2.4
Gneiss (Morimoto *et al*. 1997)		225.9	55.2	–	4.8
Gneiss (Fahrig & Bridgewater 1976)	41	225.0	60.0	57	7.5

Note: N, number of samples; *k* value of Morimoto *et al*. (1997) have not been reported.

intrusive rocks (Fig. 9d). This type of behaviour from the contact zone implies an acquisition of this component at the time of dolerite intrusion.

5 ROCK MAGNETIC EXPERIMENTS

In order to evaluate suitability of the collected samples for palaeointensity determinations, rock magnetic experiments were conducted. Stepwise IRM acquisition and thermal demagnetization of the composite IRMs acquired along three perpendicular axes (Lowrie 1990) were performed on four representative samples. IRM acquisition experiments show a complete saturation by 300 mT, indicating the dominant presence of low-coercivity magnetic minerals (Figs 10a and b). Thermal demagnetization of the composite IRMs indicates the dominant presence of low-coercivity magnetic minerals with unblocking temperature around 580 °C (Figs 10c and d). The high and medium co-ercivity fractions are almost absent.

Low field thermomagnetic analyses (K–T) were performed in air on four representative specimens using the MS2 Bartington metre (Figs 10e and f). Four other specimens were subjected to high field (Js-T) thermomagnetic analyses in helium atmosphere using the Curie Balance (Figs 10g and h). High field thermomagnetic experiments yield a reversible heating and cooling curves, indicating that no mineralogical changes has occurred during the heating phase. Although the low-field thermomagnetic analyses were performed in air, no significant difference is observed between the

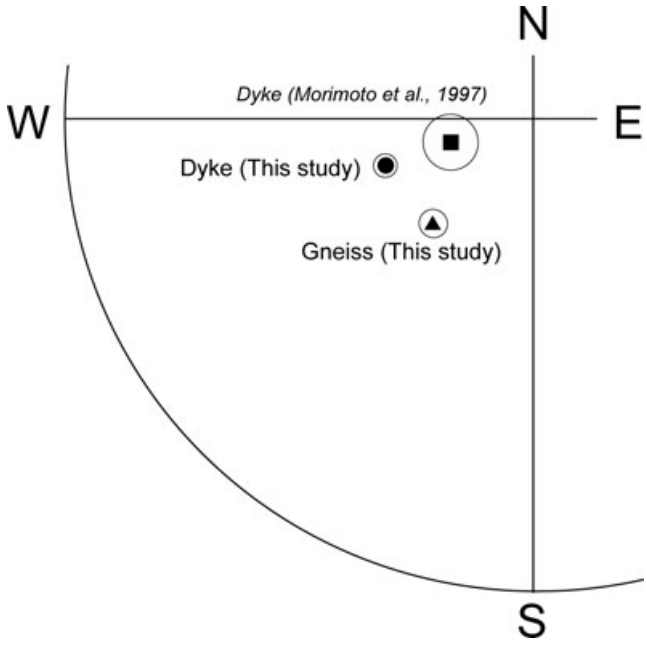

Figure 7. Comparisons of the palaeomagnetic mean directions from dolerite dykes (solid circle from this study and square from Morimoto *et al*. 1977) with direction from host gneiss through this study (triangle). Circles represent 95 per cent confidence limits.

heating and cooling curves. Both types of experiments show a Curie point between 565 and 580 °C. Rock magnetic experiments indicate titanium-poor titanomagnetite as a dominant magnetic mineral.

As a typical example (Fig. 11), hysterisis parameters were determined for four samples using the vibrating sample magnetometer. Almost similar result is obtained from all these samples. Fig. 11(b) show a display of hysteresis parameters on a Day Plot (Day *et al.* 1977), where the presence of pseudo-single domain (PSD) grains with well-clustered hysteresis properties are clearly indicated.

In order to provide further support to our interpretation, thin section microscopic observations were conducted on dolerite dyke

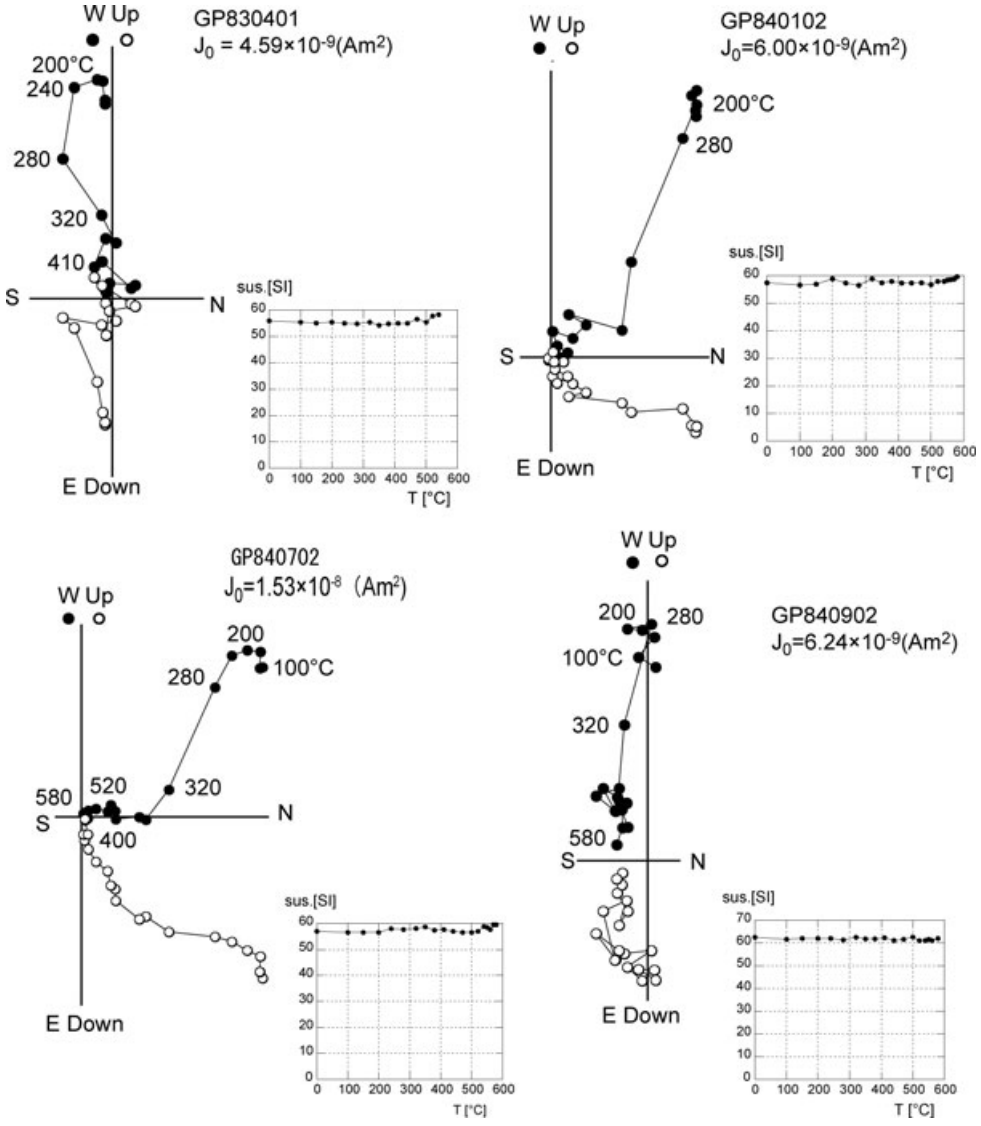

Figure 8. Results of stepwise thermal demagnetization experiments for gneiss samples collected from the contact zone: (a) result for site GP83 and (b, c, d): results for site GP84.

(Fig. 12), which indicate no sign of alteration. Texture of the grains show that some of the magnetite grains seem to have formed in biotite after its crystallization. However, these grains cannot be considered as a secondary growth, because no sign of missing iron is found in the biotite. In addition, no sign of magnetite growth under the Curie temperature is observed. These observations thus indicate magnetite related TRM as a carrier of magnetization in the dolerite rocks. Further investigations of the magnetic grain growth in volcanic rocks are needed to resolve this issue properly; however, it is out of scope for this study.

6 THELLIER'S EXPERIMENTS

6.1 Method

Coe-modified Thellier's palaeointensity experiments (Coe 1967) with pTRM checks were made on 35 samples. These samples were divided in to four sets. First set of seven pilot specimens was heated in air, and a field of 20 μT was applied along x-axis in the laboratory. Heating steps of 150, 250, 350, 450, 490, 510, 520, 530, 537, 544, 551, 558, 565, 575 and 590 °C were decided on the basis of thermal demagnetization behaviour. In order to monitor an alteration during heating (if any), pTRM checks were performed at every alternative-heating step. Second and third sets of samples (seven in each set) were heated in vacuum condition (∼5 Pa). In order to diminish any chance of thermal alteration, number of heating steps was reduced. Keeping in view the results from first set, heating steps of 250, 450, 500, 515, 530, 540, 550, 560, 570, 580 and 590 °C were chosen. Here, a pTRM check was performed at every alternative or third heating step. In order to observe the influence of field variation on intensity estimation, fields of 10 and 15 μT were applied to samples of second and third sets, respectively. For second and third sets, different pTRM steps were chosen, while magnetic field was applied along z-axis. The applied field was approximately perpendicular to the NRM direction, which was almost horizontal in sample coordinate.

The remaining 14 samples from fourth set were heated in air with applied field of 15 μT. Direction of the applied field was decided with respect to the NRM direction of each sample. In case of six samples, field parallel to NRM direction was applied, while for four

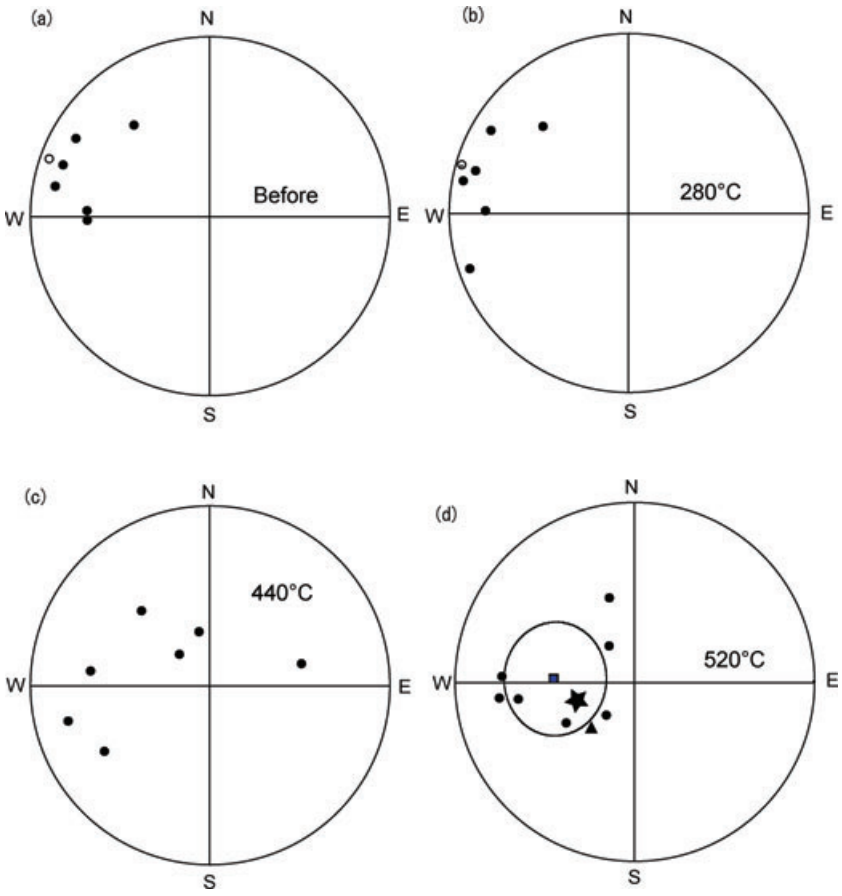

Figure 9. Palaeomagnetic directions of seven gneiss samples collected from the contact zone before (a) and after demagnetization at 280 °C (b), 440 °C (c) and 520 °C (d). Mean direction after 520 °C demagnetization step (together with alpha 95 circle) is indicated by square, while the ChRM mean direction from dyke samples is shown by star. Mean ChRM direction from gneiss samples (sites GP85 and GP86) is indicated by triangle. Solid (open) circles are projections on to lower (upper) hemisphere.

other samples antiparallel field was applied. For the remaining four samples, field perpendicular to NRM direction was applied. Heating steps of 250, 450, 500, 515, 530, 540, 550, 560, 566, 572 and 578 °C were used. The method of tail checks (Riisager & Riisager 2001) was performed, where at some temperatures (e.g. 530, 560 and 572 °C) pTRM was again demagnetized in zero field up to a temperature level at which its acquisition was made. Remanence after the first demagnetization step [NRM (Ti)] was then compared with those observed after each repeated demagnetization step [NRMre (Ti)]. Ideally, the first and repeated zero field demagnetization up to the same temperature level should result in the same remaining NRM [NRMre (Ti) -NRM (Ti) = 0].

Specimens from second to fourth sets, which were mostly taken from block samples 871 and 872, exhibit more successful results of pTRM check. Magnetic susceptibility at room temperature was monitored after each heating step.

6.2 Reliability criteria

Palaeointensity data were analysed using the ARAI plot (Nagata *et al.* 1963). Criteria listed below were used to assess the quality of experimental data.

(1) Temperature range of the linear fit has to match that of the characteristic component identified during thermal demagnetization experiments. Furthermore, the characteristic direction obtained by Thellier experiments should be within 15° to that obtained through demagnetization procedure in zero-field.

(2) The MAD value (Kirschvink 1980) for selected data should be lower than 10°.

(3) A minimum requirement of four data points should be fulfilled for a linear fit.

(4) Correlation coefficient of the segment should be larger than 0.98.

(5) A pTRM test should give a positive result for linear segment within 5 per cent of the total TRM (original TRM).

(6) At least 30 per cent of the NRM (f-fraction) has to be covered by a linear fit.

(7) Change in magnetic susceptibility should be less than 20 per cent of the original value for a temperature range of the linear segment on Arai plots.

6.3 Results

Fourteen out of thirty-five samples passed the above-mentioned criteria. Results of the palaeointensity experiments with corresponding parameters are listed in Table 3, while diagrams of the representative samples are shown in Figs 13 and 14. Mean palaeointensity obtained from 14 reliable samples is 13.9 $\pm$ 2.5 μT, where the calculated values vary between 9.4 and 17.3 μT. Although variety of conditions (such as different applied field directions and intensities)

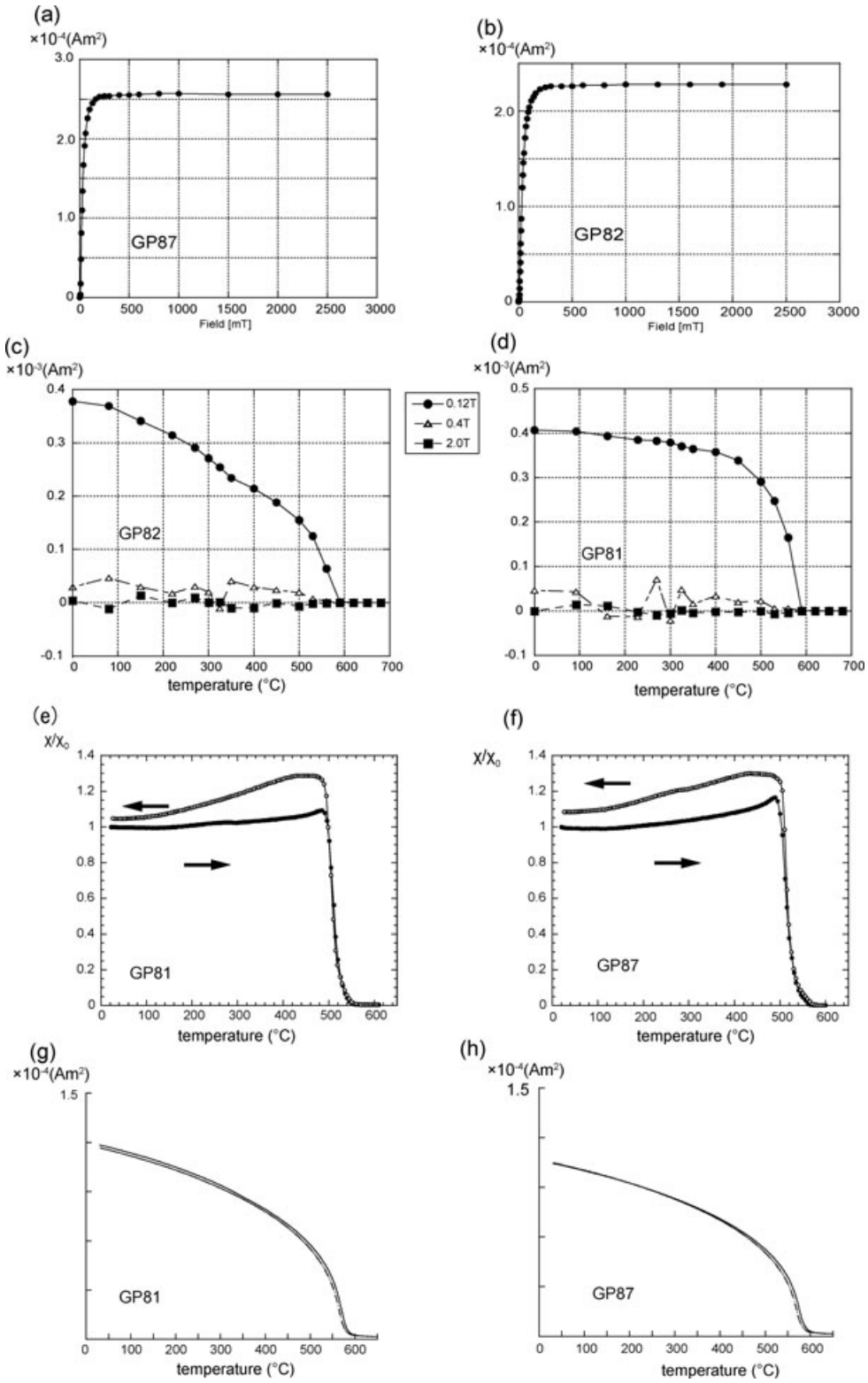

Figure 10. Typical results of rock magnetic experiments. (a) and (b) Stepwise IRM acquisition results; (c) and (d) thermal demagnetization of the composite IRMs acquired along three perpendicular axes; (e) and (f) week field thermomagnetic analyses; (g) and (h) high field thermomagnetic analyses.

have been tested during the experiments, scatter in palaeointensities appeared to be fairly small.

Most of the reliable results have been obtained from a block sample GP87. Specimens from samples GP81 and GP82 failed the pTRM check test, because the TRM value increases significantly at about 400 °C (Fig. 13d). This type of behaviour may indicate an alteration in magnetic mineralogy, although no sign of such a behaviour has been observed during the rock magnetic experiments. Difference in magnetic characteristics between these samples (GP81, GP82 and GP87) may be due to a variation in sampling

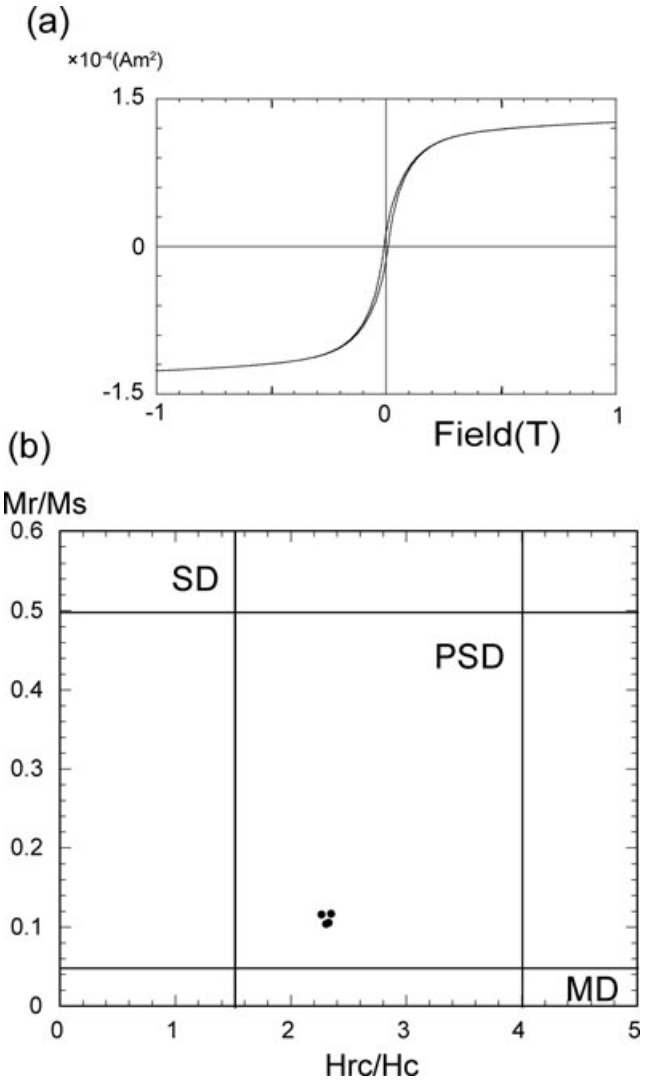

Figure 11. (a) A typical example of hysterisis curve for dolerite sample. (b) Hysterisis parameters on Day plot for dolerite samples.

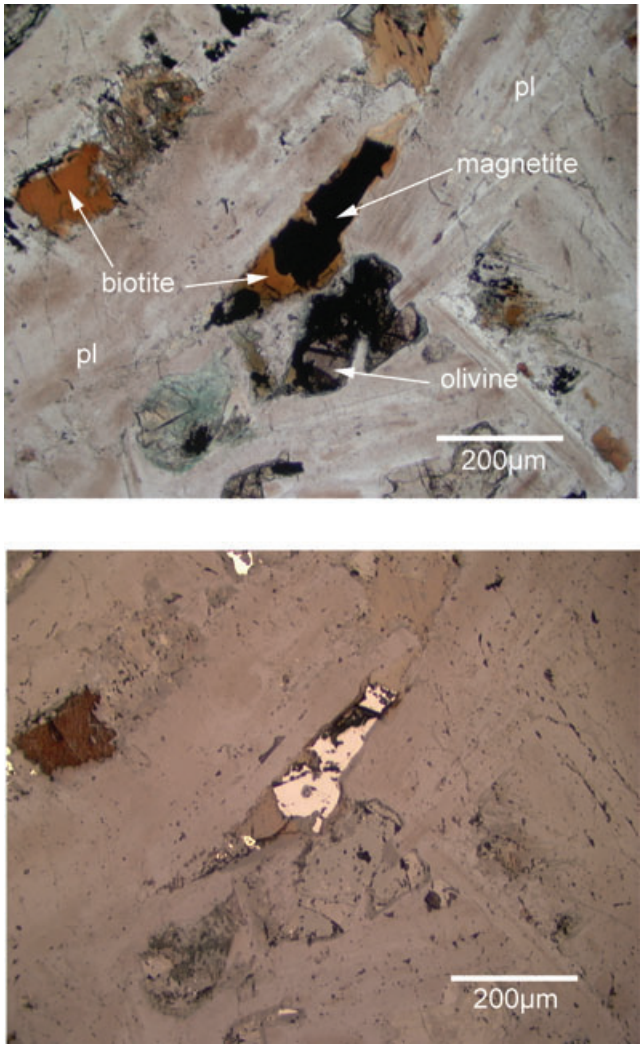

Figure 12. Photomicrograph of specimen from dolerite dyke (GP871–101). Magnetite is observed in biotite crystal. (a) Transmitted light and (b) reflected light.

localities. Results obtained under air (1st and 4th sets) and vacuum conditions (second and third sets) are not significantly different.

In some samples, the demagnetization paths don't follow a straightforward decay to the origin, and laboratory induced TRM could not be completely demagnetized. Using the method of Selkin & Tauxe (2000) and Tanaka & Kobayashi (2003), a difference angle 'θ' between the principal component (corresponding to the selected linear segment) and the direction of the mass centre is calculated. Out of fourteen reliable samples, we have chosen another data set of nine samples that have θ value less than 15°. These nine samples fulfil the grade-A level criteria of Tauxe & Staudigel (2004). Mean palaeointensity of this data set (13.6 $\pm$ 2.9 μT) is not significantly different from that of fourteen samples (13.9$\pm$2.5 μT). Mean palaeointensity (13.4 μT) calculated from samples with much smaller θ value (<8°) is also not significantly different from this value of 13.9 $\pm$ 2.5 μT. Moreover, another mean value (13.9 μT) obtained from only three samples using more strict criteria of data selection (Kissel & Laj 2004) is also in agreement with that from fourteen samples. This type of behaviour clearly indicates that no large shift in intensity value is observed as a result of variation in θ value or selection criteria.

As mentioned above, an uncleaned part of the TRM may be due the presence of MD grains in the studied samples. Day plots of hysteresis experiments for representative samples indicate a PSD character (Day *et al*. 1977), however, a zone of PSD grains has been interpreted as a mixture of MD and SD grains (Dunlop 2002). In order to evaluate the effects of tail on the remaining TRM, results from pTRM–tail check of fourth experiment are examined here. The pTRM tails from MD grains take a maximum value when laboratory induced field direction is antiparallel to the NRM direction (e.g. Yu & Dunlop 2003). As shown in Figs 14(c) and (d), the tail [NRMre (Ti)] – [NRM (Ti)] obtained from the sample with antiparallel field is still less than 10 per cent of the initial intensity (before demagnetization). Although, reliability of intensity data from samples with perpendicular field is questionable because of unsuccessful pTRM check, we have calculated tail parameter normalized to NRM ($\delta\tau^*$; Leonhardt *et al*. 2004), where $\delta\tau^*$ value is 2.6 and 4.2 for antiparallel field and 2.9 and 2.6 for perpendicular field (two samples). These $\delta\tau^*$ values are reasonably small, indicating that the influence of MD grains is not high enough to produce significant bias in the intensity results.

Table 3. Palaeointensity results.

Sample	Fl (μT)	Field direction	Set	Furnace	TR (°C)	n	b	σb	r	f	g	q	θ	MAD	$F \pm \Delta F$ **μT**
GP871141	20	x-axis	A	Air	250–558	11	−0.682	0.025	−0.995	0.5070	0.8501	5.8790	15.8	5.8	13.6 ± 0.5
GP871072	20	x-axis	A	Air	490–558	8	−0.647	0.047	−0.984	0.6760	0.8725	16.2400	18.8	6.6	12.9 ± 0.9
GP872062	20	x-axis	A	Air	250–558	11	−0.672	0.039	−0.985	0.6108	0.8912	9.3299	19.3	5.2	13.4 ± 0.8
GP871–81[a]	10	z-axis	B	Vacuum	250–560	8	−1.682	0.064	−0.996	0.4335	0.8268	9.4843	6.2	7.9	16.8 ± 0.6
GP871–91[a]	10	z-axis	B	Vacuum	250–560	8	−1.481	0.069	−0.993	0.5035	0.8373	8.9946	8.0	8.1	14.8 ± 0.7
GP871–22[b]	10	z-axis	B	Vacuum	250–560	8	−1.278	0.110	−0.978	0.4817	0.8275	4.6203	12.6	4.3	12.8 ± 1.1
GP871–112	15	z-axis	C	Vacuum	450–540	5	−1.013	0.047	−0.997	0.3697	0.7335	5.7890	15.9	4.3	15.2 ± 0.7
GP871–131	15	z-axis	C	Vacuum	450–550	6	−1.150	0.120	−0.978	0.3128	0.7393	2.2068	17.3	6.2	17.3±1.8
GP871–121[b]	15	z-axis	C	Vacuum	250–540	6	−1.043	0.082	−0.988	0.3931	0.7876	3.9374	14.3	9.1	15.6 ± 1.2
GP871–142[c]	15	Parallel	D	Air	250–540	6	−0.625	0.016	−0.999	0.3620	0.7840	11.1780	6.7	3.9	9.4 ± 0.2
GP871–111[a]	15	Parallel	D	Air	250–540	6	−0.657	0.053	−0.987	0.3164	0.7655	2.9816	5.2	6.2	9.9 ± 0.8
GP871–51[c]	15	Antiparallel	D	Air	250–540	6	−1.074	0.020	−0.999	0.5171	0.7903	21.6277	6.2	5.3	16.1 ± 0.3
GP871–101[c]	15	Antiparallel	D	Air	250–550	7	−1.079	0.056	−0.993	0.5306	0.8215	8.3777	3.1	6.3	16.2 ± 0.8
GP871–31[a]	15	Parallel	D	Air	250–550	7	−0.727	0.058	−0.984	0.3711	0.8115	3.7753	1.5	7.6	10.9 ± 0.9

Notes: Fl, laboratory field strength; field direction, direction of the laboratory field [x-, y-, z-axis direction of the sample frame; parallel (antiparallel), parallel (antiparallel direction to the NRM of rock samples)]; set, sample sets of experiments; furnace, atmosphere in the furnace; TR, temperature range for the linear segment; n, number of data point included in the linear regression; b, slope of the segment; σb, standard error of b; r, correlation coefficient of the linear relationship; f, g, q, quality parameters after Coe *et al*. (1978); θ, different angle of the selected NRM component from the origin on the orthogonal plot after Tanaka *et al*. (2003); MAD, quality parameter of the linearity after Kirschvink (1980); F, ΔF, palaeointensity and its standard error.
[a]Samples which pass $\theta < 8°$ criteria.
[b]Samples which pass $\theta < 15°$ criteria.
[c]Samples which pass the criteria of Kissel & Laj (2004).

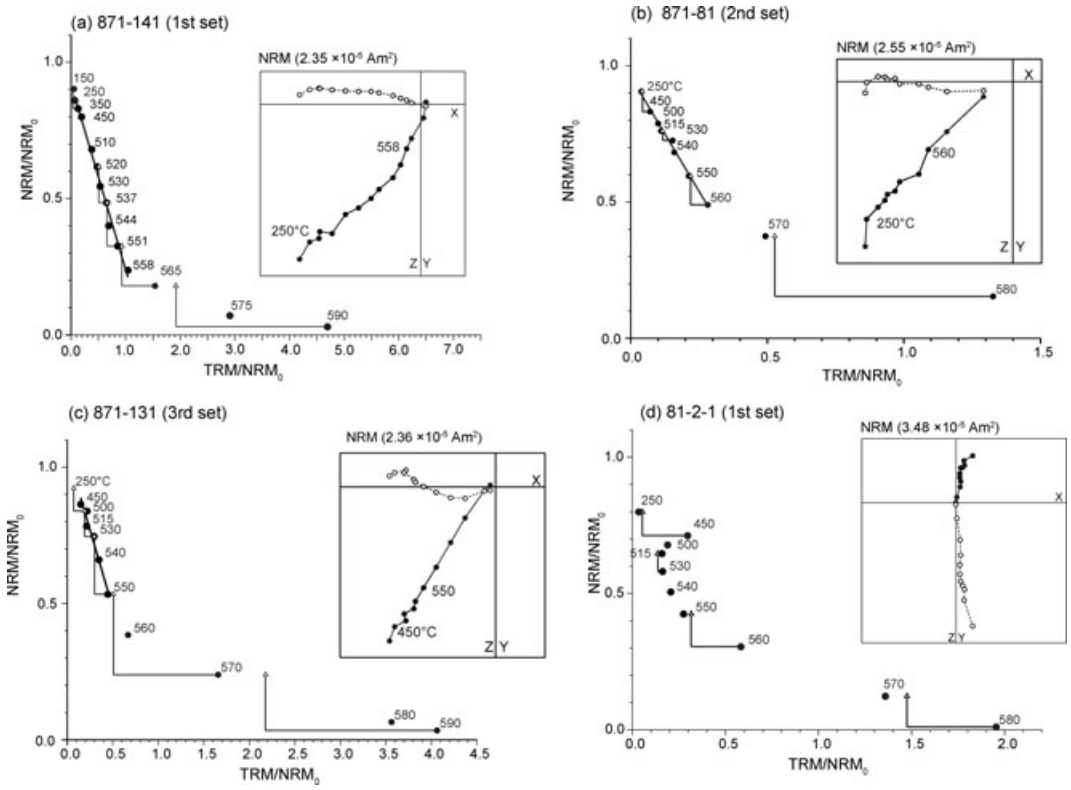

Figure 13. Typical examples of the first (a), second (b) and third (c) set of palaeointensity determination. In orthogonal vector plots the open and solid symbols indicate projections on to horizontal and vertical planes, respectively. (d) Result in this diagram shows a failure to determine palaeointensity.

In order to further investigate the effects of MD grains on intensity, results of the Thellier experiments from fourth set have been simulated with computer generated phenomenological numerical model (Biggin 2006). His parameters of the typical MD samples (ms = 1, $\alpha_1 = 1$, $\alpha_2 = 0.8$, $\alpha_3 = 0.8$, $\alpha_4 = -0.35$ and $\lambda = 0.2$) are used here. Experimental procedures and applied field direction with respect to NRM direction are chosen according to the experiments of our fourth set. Intensities of fields used for imparting NRM ($H_{\rm nrm}$) and for partial remagnetization treatment ($H_{\rm lab}$) are set to be compatible. Models produced through Arai plots exhibit a concave shape feature (Fig. 15). Palaeointensity value calculated from the left side of the Arai plot is larger than the ideal value. A

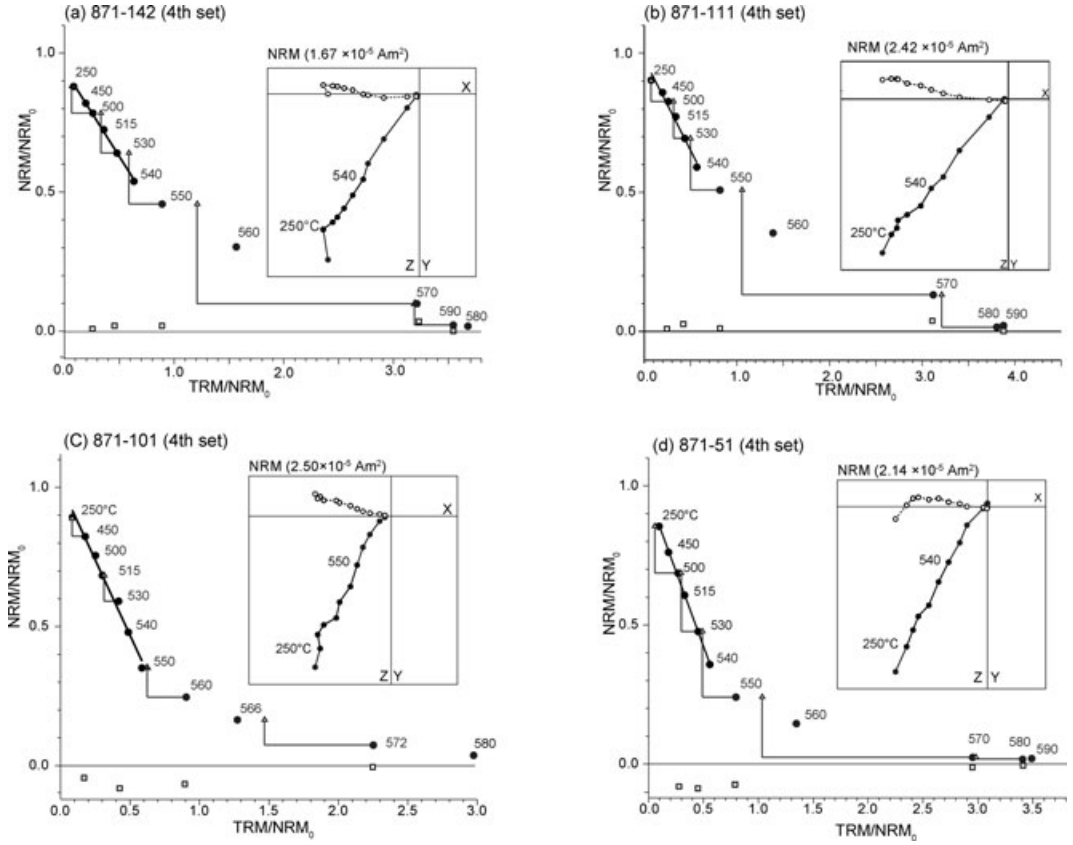

Figure 14. Typical examples from fourth set of palaeointensity determination. Open squares show results from tail check. (a) and (b) Applied field is parallel to the NRM of sample; (c) and (d) applied field is antiparallel to the NRM of sample.

slope calculated for six points is 1.18 for parallel experiment and 1.28 for antiparallel experiment, while the value of ideal SD grain has to be 1.0. A concave shape spectra obtained from our Thellier results may be partly due to the effect of MD grain, although large TRM value above 560°C seems to have resulted from thermally induced alteration as judged from the failure of pTRM check. A difference in calculated intensities between the MD model and that of the ideal value is larger when field is applied antiparallel to the NRM direction. In our case, three intensity values from parallel field experiments are about 30 per cent lower than those obtained from antiparallel experiments. Although, the number of samples is not fair enough to clearly project this distinction, a difference in intensity values with respect to field directions may be due to pTRM-tail. In this connection, a mathematical model by Yu *et al*. (2004) also indicates a difference in intensity values with changing field direction.

The mean intensity obtained from 14 samples ($13.9 \pm 2.5\ \mu$T) is significantly smaller than that of the present-day Earth's field in the study area (55.2 μT; IGRF 2005). A simulation based numerical model suggests that the effect of MD grain would tend to make palaeointensity higher. If true, an intensity value of 13.9 μT from this study may also include some overestimation. It is therefore concluded that rather small value of palaeointensity was the characteristic of geomagnetic field at the time of dyke intrusion in the study area. As reported by Biggin *et al*. (2007), variation in cooling rate might cause an underestimation of palaeointensity in the non-SD material. However, samples used for this study have been collected from the margin of the dyke, which is spread over a limited zone of several 10s m wide. As a result, the effects of cooling rate variation on our samples seem to be negligible. Macouin *et al*. (2003) have also found no influence of cooling rate variation on 250-m-wide Proterozoic mafic dyke.

7 DISCUSSION AND INTERPRETATION

7.1 Age of the dolerite dykes

Evidence of dyke penetration through a boundary between the Akila and Akulleq terranes clearly indicates that intrusion of dolerite took place after the amalgamation of the Archaean terranes. The time of this assembly has been estimated by Friend *et al.* (1996) using the SHRIMP U-Pb zircon geochronology. An oldest geological event experienced by all three terranes in this area is the high-grade metamorphism, which has been dated at ∼2720 Ma using the zircon results (Friend *et al.* 1996). The process of amalgamation for these terranes has been placed just before the commencement of this metamorphic event. An estimated time for dyke intrusion (2585 ± 21 Ma) obtained from ^{40}Ar/^{39}Ar results (this study) is fairly consistent with the above-mentioned interpretation. Lack of metamorphic features in the studied dykes suggests that no significant geological event (including metamorphism) has occurred after the process of dyke intrusion. These informations therefore suggest that amalgamation of the cratonic terranes and the process of high-grade metamorphism (∼2720 Ma) were followed by an intrusion of the studied dyke. K-Ar ages of 2707 ± 76 Ma and 2796 ± 72 Ma (mean: 2752 Ma) have also been reported (Morimoto *et al.* 1997) from another dolerite dyke in the Nuuk town, about 15 km north of this study area. This large window of ages from Nuuk area may suggest

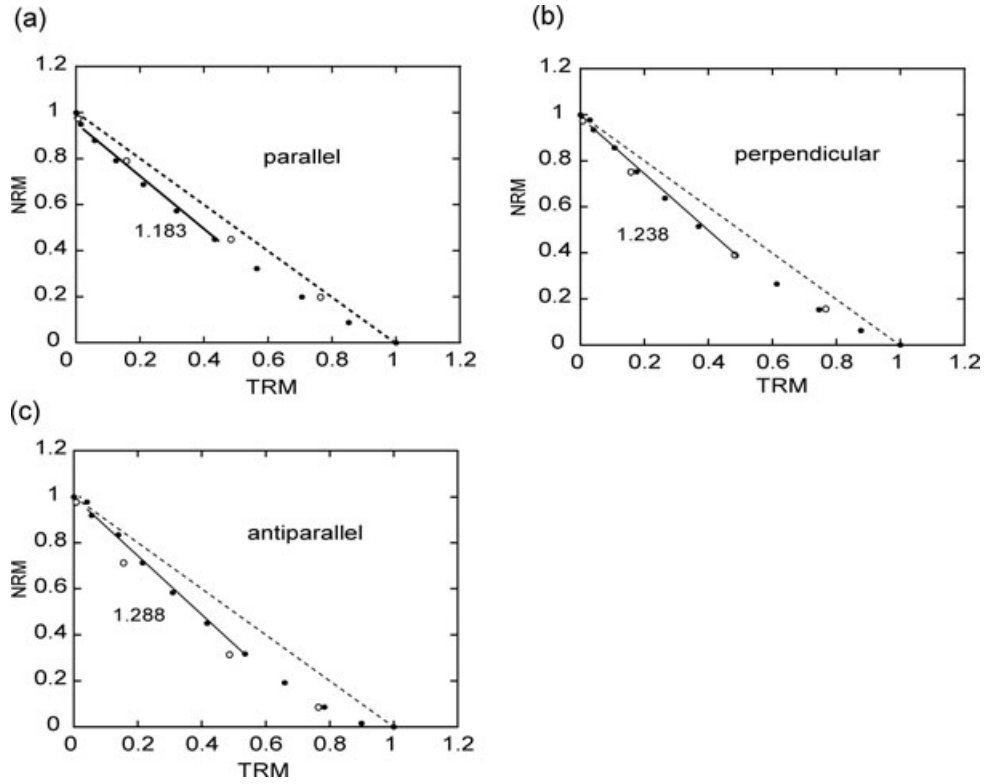

Figure 15. Arai plots produced by the phenomenological model (Biggin 2006) for MD-like samples. Experimental profiles for making this model are made from our Thellier Experiments with pTRM check: Although temperature intervals are constant in these models, procedure and steps of partial magnetization and demagnetization follows our actual Thellier experiments. (a) Applied field is parallel to initial TRM direction. (b) Applied field is perpendicular to initial TRM direction. (c) Applied field is antiparallel to initial TRM direction. Open circles represent steps for pTRM check. Solid lines represent a line fit for second to seventh thermal steps.

a continuation of dolerite intrusions for fairly long period of time after the completion of amalgamation. However, additional data are needed to fully understand these processes in such old Precambrian rocks. K-Ar dating of 2796 Ma by Morimoto *et al.* (1997), which is clearly older than the age of metamorphism (at 2720 Ma) in the study area, can be considered as over estimation.

7.2 Palaeomagnetic direction

Palaeomagnetic pole obtained from the here studied dolerite dyke (Fig. 16) is compared with the Archaean to early Proterozoic poles of the Laurentia. Since, the dolerite dyke has vertically intruded the host gneisses; it is presumed that no significant tilting of the studied rocks has occurred since their intrusion. A palaeomagnetic pole position is calculated after rotating Greenland by 18° back to North America about the Euler pole of 70.5°N, 94.4°W (Bullard *et al*. 1965). A palaeomagnetic pole obtained from the dyke samples (31.6°N and 92.9°W) give a position close enough to other Early Proterozoic poles from Laurentia. Pole position from this study is also close to a pole reported by Morimoto *et al.* (1997) from another dolerite dyke in the Nuuk area. Since, pole position from single dyke could be influenced by secular variation and/or local rotation; it may not be taken as a representative of palaeomagnetic pole. In order to ascertain whether the characteristic component from dyke samples is of primary or secondary origin, we compared the corresponding pole with the latest APWPs of Laurentia, that is, the Proterozoic APWP (Borradaile *et al*. 2003) and the Phanerozoic APWP (McElhinny & McFadden 2000). The here obtained pole position from dolerite dyke (both before and after rotating back) present no agreement with any of these APWPs. This divergence in pole positions thus supports a primary origin for magnetization in the dyke samples.

7.3 Palaeointensity

Rather small palaeointensity is the characteristic of the dolerite dyke. A virtual dipole moment (VDM) calculated from mean palaeointensity and the observed mean inclination (+62.6°) is $2.30 \pm 0.42 \times 10^{22}$ Am^2, which is about one quarter of the present-day Earth's field intensity.

According to previously reported results, it has been suggested that some of the low VDM values during the Proterozoic era may be due to the influence of thermochemical remanent magnetization (TCRM; Smirnov & Tarduno 2005). Based on this idea, a characteristic component obtained from the Matachewan Dyke swarm (about 2.5 Ga old) has been ascribed as a TCRM. They have estimated intensity of this TCRM from a narrow temperature range (between 520 and 580 °C), which is about 25 per cent of the true TRM intensity. A temperature range of ∼450 to 580 °C for the ChRM component in this study is fairly broader than the one reported from the Matachewan dyke. Although, the VDM values from both these data sets are almost similar, intensity value from this study is regarded as that of the TRM rather than TCRM.

Low VDM value, rather than a secular variation, appears to be a characteristic of the Earth's magnetic field at 2.6–2.7 Ga. Almost similar VDM value of about $1.9 \pm 0.6 \times 10^{22}$ Am^2 has also been

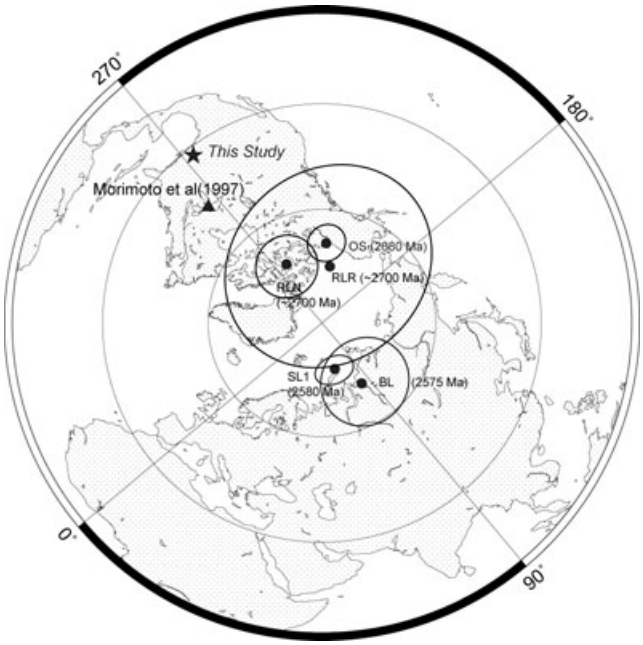

Figure 16. Palaeomagnetic pole position of the dolerite dyke from this study (solid star) together with those reported from 2.5 to 2.7 Ga rock units of North America with 95 per cent confidence ellipses. RLN and RNR: Red Lake greenstone of ∼2700 Ma (Constanzo-Alvarez & Dunlop 1993); OS: Otto stock of 2680 Ma (Pullaiah & Irving 1975); SL1: Shelley Lake granite, 2580 Ma (Dunlop 1984a); BL: Burchell Lake granite (Dunlop 1984b).

reported from another Archaean dyke in the study area (Morimoto *et al.* 1997). A difference between the present-day VDM and those obtained from two dykes is too large to be explained by any significant event in terms of secular variation.

Our new data preciously assign this low VDM value to a period much before the 2.5 Ga. Availability of reliable palaeointensity data prior to 2.5 Ga is very limited. Fig. 17 shows only those Archaean–Proterozoic VDM data that passed a criteria of Macouin *et al.* (2006), including a double heating technique with pTRM checks.

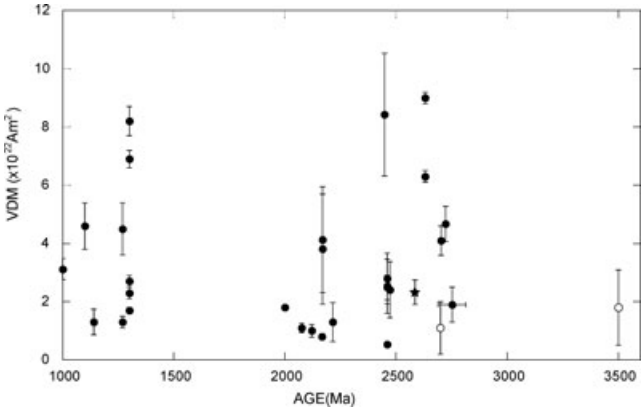

Figure 17. Diagram showing variation of virtual dipole moment (VDM) versus age data. Data used here are those summarized by Macouin *et al*. (2006) together with results from this study. The summarized data are from Morimoto *et al*. (1997), Yoshihara & Hamano (2000, 2004), Selkin *et al*. (2000), Sumita *et al*. (2001), Yu & Dunlop (2001, 2002); Smirov *et al* (2003), Macouin *et al*. (2003), Halls *et al.* (2004), Macouin *et al*. (2006), McArde *et al.* (2004), Thomas & Piper (1995) and Biggin *et al*. (2009). Closed star indicates result from this study and open circles represent secondary magnetization.

A type of data recognized as a primary TRM with low intensity value (less than 3×10^{22} Am^2) at or before 2631 Ma VDM peak (Yoshihara & Hamano 2000) is only available from two areas of Greenland (this study and that of Morimoto *et al.* 1997). The oldest data with low VDM value is only reported from 3.5 Ga komatiite, however, their source of acquisition has been declared as a CRM (Yoshihara & Hamano 2004). A VDM record between 3.5 and 2.7 Ga is still lacking. In fact, data from Greenland seems to be the only available option that documents record of ancient geomagnetic field prior to the onset of modern geodynamo, which has been reported to be instigated by a nucleation of solid inner core before the Early Proterozoic (Hale 1987, Smirnov *et al.* 2003).

Low VDM values have also been reported from the middle Proterozoic rocks. As compared to present-day geomagnetic field, a mean VDM value reported by Macouin *et al*. (2006) from Precambrian rocks (3.1×10^{22} Am^2) is obviously lower in strength. An intensity of the Earth's magnetic field has increased by a factor of 4 between 2.7 and 2.5 Ga (during a period of 200 Myr). The strength of VDM similar to that of the present-day field has been observed around 2.5 Ga (Yoshihara & Hamano 2000; Smirnov *et al.* 2003). Breuer & Spohn (1995) have suggested a flush instability in the mantle convection around the Archaean–Proterozoic transition. Relatively high strength of geomagnetic field around 2.5 Ga might have occurred as a result of this flush instability rather than a record of nucleation in the inner core.

ACKNOWLEDGMENT

We are grateful for Dr H. Tanaka for fruitful discussion and extensive support. As a result of his courtesy, Thellier experiments and K-T analyses were made in the laboratory at Faculty of Education, Kochi University. Js-T and hysterisis experiments were carried out in the Center for Advanced Marine Core Research, Kochi University, and we are grateful to Kazuto Kodama for use of rock magnetic facilities. Constructive and detailed reviews of Dr A. Biggin and Dr P. Selkin and helpful comments from Editor Dr C. Langereis largely improved this manuscript. We thank Dr Y. Yamamoto for his useful discussion. This research was partly supported by the Toyota Foundation and Grant-in aid (No. 18403012) from MEXT.

REFERENCES

Biggin, A.J., 2006. First-order symmetry of weak-field partial thermoremanence in multi-domain (MD) ferromagnetic grains: 2. Implications for Thellier-type palaeointensity determination, *Earth planet. Sci. Lett.,* **245,** 454–470.

Biggin A.J., Perrin, M. & Dekkers M.J., 2007. A reliable absolute palaeointensity determination obtained from a non-ideal recorder, *Earth planet. Sci. Lett.,* **257,** 545–563.

Biggin, A.J., Strik, G.H.M.A. & Langereis, C.G., 2009. The intensity of geomagnetic field in the late-Archaean: new measurements and an analysis of the updated IAGA palaeointensity database, *Earth Planets Space,* **61,** 9–22.

Borradaile, Graham J., Werner, Tomasz & Lagroix, France, 2003. Differences in paleomagnetic interpretations due to the choice of statistical, demagnetization and correction techniques: Kapuskasing Structural Zone, northern Ontario, Canada, *Tectonophysics,* **363,** 103–125.

Breuer, D. & Spohn, T., 1995. Possible flush instability in mantle convection at the Archaean-Proterozoic transition, *Nature,* **378,** 608–610.

Bridgewater, D., Keto, L., McGregor, V.R. & Myers J.S., 1976. Archaean Gneisscomplex of Greenland, in *Geology of Greenland,* pp. 19–75, eds Escher, A. & Watt, W. S., Geological Survey of Greenland, Copenhagen.

Bullard, E.C., Everett, J.E. & Smith, A.G., 1965. The fit of the continents around the Atlantic, *Philos. Trans. R. Soc. Lond., A.,* **258,** 41–51.

Coe, R.S., 1967. Paleo-intensities of Earth's magnetic field determined from Tertiary and Quaternary rocks, *J. geophys. Res.,* **72,** 3247–3262.

Coe, R.S., Gromme, S. & Mankinen, E.A., 1978. Geomagnetic paleointensities from radiocarbon-dated lava flows on Hawaii and the question of the Pacific nondipole low, *J. geophys. Res.,* **83,** 1740–1756.

Constanzo-Alvarez, V. & Dunlop, D.J., 1993. Paleomagnetism of the Red Lake greenstone belt, northwestern Ontario: possible evidence for the timing of gold mineralization, *Earth planet. Sci. Lett.,* **119,** 599–615.

Day, R., Fuller, M., Schmidt, V.A., 1977. Hysteresis properties of titanomagnetites: grain size and composition dependence, *Phys. Earth planet. Inter.,* **13,** 260–267.

Dunlop, D.J., 1984a. Paleomagnetism of Archaean rocks from northwestern Ontario: II, Shelly Lake granite, Quetico Subprovince, *Can. J. Earth Sci.,* **21,** 869–878.

Dunlop, D.J., 1984b. Paleomagnetism of Archean rocks from northwestern Ontario: IV, Burchell Lake granite, Wawa-Shebandowan Subprovince, *Can. J. Earth Sci.,* **21**: 1098–1104.

Dunlop, D.J., 2002. Theory and application of the Day plot (M_{rs}/M_s versus H_{cr}/H_c). 1: theoretical curves and tests using titanomagnetite data, *J. geophys. Res.* **107(** B3), doi:10.1029/2001JB000486.

Escher, A. & Watt, W.S. (eds), 1976. *Geology of Greenland,* The Geological Survey of Greenland, Copenhagen.

Fahrig, W.F. & Bridgewater, D., 1976. Late Archean-Early Proterozoic paleomagnetic pole positions from West Greenland, in *The Early History of the Earth,* ed. Windley, B. F., pp 427–439, John Wiley and Sons, London.

Friend, C.R.L., Nutman, A.P. & McGregor, V.R., 1988. Late Archaean terrane accretion in the Godthåb region, Southern West Greenland, *Nature,* **335,** 535–538.

Friend, C.R.L., Nutman, A.P., Baadsgaard, H., Kinny, P.D. & McGregor, V.R., 1996. Timing of late Archaean terrane assembly, crustal thickening and granite emplacement in the Nuuk region, southern West Greenland, *Earth planet. Sci. Lett.,* **142,** 353–365.

Hale, C.J., 1987. Palaeomagnetic data suggest link between the Archean-Proterozoic boundary and inner-core nucleation, *Nature,* **329,** 233–237.

Halls, H.C., McArde, N.J., Gratton, M.N., Hill, M.J. & Shaw, J., 2004. Microwave paleointensities from dyke chilled margins: a way to obtain long-term variations in geodynamo intensity for the last three billion years, *Phys. Earth planet. Inter.,* **147,** 183–195.

Hyodo, H., Matsuda, T., Fukui, S. & Itaya, T., 1994. $^{40}Ar/^{39}Ar$ age determination of a single mineral grain by Laser step heating, *Bull. Res. Inst. Nat.,* Okayama Univ. of Sci., **20,** 63–67.

Hyodo, H., Itaya, T. & Matsuda, T., 1995. Temperature measurement of small minerals and its precision using Laser heating, *Bull. Res. Inst. Nat.,* Okayama Univ. Sci., **21**, 3–6.

Hyodo, H., Kim, S., Itaya, T. & Matsuda, T., 1999. Homogeneity of neutron flux during irradiation for $^{40}Ar/^{39}Ar$ age dating in the research reactor at Kyoto University, *J. Miner. Petrol. Econ. Geol.,* **94,** 329–337.

Kalsbeek, F. &.Taylor, P.N., 1985. Age and origin of early Proterozoic dolerite dykes in South-West Greenland, *Contrib. Miner. Petrol.,* **89,** 307–316.

Kissel, C. & Laj, C., 2004. Improvements in procedure and paleointensity selection criteria(PICRIT-03) for Thellier and Thellier determinations: application to Hawaiian basaltic long cores, *Phys. Earth planet. Inter.,* **147,** 155–169.

Kirschvink, J.L., 1980. The least-squares line and plane and the analysis of paleomagnetic data, *Geophys. J. R. astr. Soc.,* **62,** 699–718.

Lee, J.K. W., Onstott, T.C. & Hanes, J.A., 1990. An $^{40}Ar/^{39}Ar$ investigation of the contact effects of a dyke intrustion, Kapuskasing Structural Zone, Ontario, *Contrib. Miner. Petrol.,* **105,** 87–105.

Leonhardt, R., Heunemann, C. & Krása, D., 2004. Analyzing absolute paleointensity determinations: acceptance criteria and the software ThellierTool4.0, *Geochem. Geophys. Geosyst.,* **5,** Q12016, doi:10.1029/2004GC000807.

Lowrie, W., 1990. Identification of ferromagnetic minerals in a rock by coercivity and unblocking temperature properties, *Geophys. Res. Lett.,* **17,** 159–162.

Macouin, M., Valet, J.P., Besse, J., Buchan, K., Ernst, R., LeGoff, M. & Scharer, U., 2003. Low paleointensities recorded in 1 to 2.4 Ga Proterozoic dykes, Superior Province, Canada. *Earth planet. Sci. Lett.,* **213,** 79–95.

Macouin, M., Valet, J.P., Besse, J. & Ernst R.E., 2006. Absolute paleointensity at 1.27 Ga from the Mackenzie dyke swarm (Canada), *Geochem. Geophys. Geosyst.,* **7**(1), Q01H21, doi:10.1029/2005GC000960.

McArde, N.J., Halls, H.C. & Shaw, J., 2004. Rock magnetic studies and a comparison between microwave and Thellier paleointensities for Canadian Precambrian dykes, *Phys. Earth planet. Inter.,* **147,** 247–254.

McElhinny, M.W. and McFadden, P.L., 2000. *Paleomagnetism: Continents and Ocean,* Academic Press.

Morimoto, C., Otofuji, Y., Miki, M., Tanaka, H. & Itaya, T., 1997. Preliminary palaeomagnetic results of an Archaean dolerite dyke of west Greenland: geomagnetic field intensity at 2.8 Ga, *Geophys. J. Int.,* **128,** 585–593.

Nagata, T., Arai, Y. & Momose, K., 1963. Secular variation of the geomagnetic total force during the last 5000 years, *J. geophys. Res.* **68,** 5277–5281.

Nielsen, T.F.D., 1985. Mafic dyke swarms in Greenland: a review, in *Mafic dike Swarms, Geol. Assoc. Canada Spec. Pap.,*Vol. 34, pp. 349–360, eds Halls, H. C. & Fahrig, W. F..

Nutman, A.P., Friend, C.R.L., Baadsgaarf, H. & McGregor, V.R., 1989. Evolution and assembly of Archean gneiss terranes in the Godthåbsfjord region, southern west Greenland: structural, metamorphic, and isotopic evidence, *Tectonics,* **8,** 573–589.

Pullaiah, G. & Irving, E., 1975. Paleomagnetism of the contact aureole and late dikes of the OttoStock, Ontario, and its applications to early Proterozoic apparent polar wandering, *Can. J. Earth Sci.,* **12,** 1609–1618.

Riisager, P., Riisager, J., 2001. Detecting multidomain magnetic grains in Thellier paloeointensity experiments, *Phys. Earth Planet. Inter.,* **125,** 111–117.

Roddick, J.C., 1983. High precision intercalibration of ^{40}Ar-^{39}Ar standards, *Geochim. Cosmochim. Acta,* **47,** 887–898.

Selkin, P.A. & Tauxe, L., 2000. Long-term variations in palaeointensity. *Philos. Trans. R. Soc. Lond. A,* **358,** 1065–1088.

Selkin, P.A., Gee, J.S., Tauxe, L., Meurer, W. P. & Newell, A.J., 2000. The effect of remanence anisotropy on paleointensity estimates: a case study from the Archean Stillwater complex, *Earth planet. Sci. Lett.,* **183,** 403–416.

Smirnov, A.V. & Tarduno, J.A., 2005. Thermochemical remanent magnetization in Precambrian rocks: are we sure the geomagnetic field was weak? *J. geophys. Res.,* **110,** B06103, doi:10.1029/2004JB003445.

Smirnov, A.V., Tarduno, J.A. & Pisakin B.N., 2003. Paleointensity of the early geodynamo (2.45 Ga) as recorded in Karelia: a single-crystal approach, *Geology,* **31,** 415–418.

Stevenson, D.J., Spohn, T. & Schubert, G., 1983. Magnetism and thermal evolution of terrestrial planets, *Icarus,* **54,** 466–489.

Sumita, I., Hatakeyama, T., Yoshihara, A. & Hamano, Y., 2001. Paleomagnetism of late Archean rocks of Hamersley basin, Western Australia and the paleointensity at early Proterozoic, *Phys. Earth planet. Inter.,* **128,** 223–241.

Tanaka H. & Kobayashi, T., 2003. Paleomagnetism of the latte Quaternary Ontake Volcano, Japan: directions, intensities, and excursions, *Earth Planets Space,* **55,** 189–202.

Tauxe, L. & Staudigel, H., 2004. Strength of the geomagnetic field in the Cretaceous Normal Superchron: new data from submarine basaltic glass of the Troodos Ophiolite, *Geochem. Geophys. Geosyst.,* **5,** Q02H06, doi:10.1029/2003GC000635.

Thomas, D.N. & Piper, J.D.A., 1995. Evidence for the existence of a transitional geomagnetic field record in a Proterozoic lava succession, *Geophys. J. Int.,* **122,** 266–282.

Yoshihara, A. & Hamano, Y., 2000. Intensity of the Earth's magnetic field in late Archean obtained from diabase dikes of the Slave Province, Canada, *Phys. Earth planet. Inter.,* **117,** 295–307.

Yoshihara, A. & Hamano, Y., 2004. Paleomagnetic constraints on the Archean geomagnetic field intensity obtained from komatiites of the Barberton and Belingwe greenstone belts, South Africa and Zimbabwe, *Precambrian Res.,* **131,** 111–142.

Yu, Y. & Dunlop, D.J., 2001. Paleointensity determination on the late Precambrian Tudor Gabbro, Ontario. *J. geophys. Res.* **106,** 26 331–26 343.

Yu, Y. & Dunlop, D.J., 2002. Multivectorial paleointensity determination from the Cordova Gabbro, southern Ontario. *Earth planet. Sci. Lett.,* **203,** 983–998.

Yu, Y. & Dunlop, D.J., 2003. On partial thermoremanent magnetization tail checks in Thellier paleointensity determination. *J. geophys. Res.* **108** (B11), doi:10.1029/2003JB002420.

Yu, Y., Tauxe, L. & Genevey, A., 2004. Towards an optimal geomagnetic field intensity determination technique. *Geochem. Geophys. Geosyst.* **5**(2), Q02H07, doi:10.1029/2003GC000630.